ADVANCED ELECTRONIC MATERIALS
www.advelectronicmat.de

Sunlight-Triggerable Transient Energy Harvester and Sensors Based on Triboelectric Nanogenerator Using Acid-Sensitive Poly(phthalaldehyde)

*Changsheng Wu, Jisu Jiang, Hengyu Guo, Xianjie Pu, Lisha Liu, Wenbo Ding, Paul A. Kohl, and Zhong Lin Wang**

Transient electronics that disintegrate via material dissolution or depolymerization under certain stimuli have great potential in biomedical and military applications. The triboelectric nanogenerator (TENG), an emerging mechanical energy harvesting technology with great flexibility in material choices, is promising in offering transient power sources. Previously reported transient energy harvesters using biodegradable polymers require solution-based degradation and have limited applications in non-biological scenarios. A short time span, sunlight-triggered degradable TENG is developed. The main substrate includes an acid-sensitive poly(phthalaldehyde) (PPHA), a photoacid generator (PAG), and a photosensitizer (PS). Through photo-induced electron transfer, the ultraviolet radiation absorbed by the PS is transferred to the PAG to generate photoacids that trigger the depolymerization of PPHA. Transient TENG-based mechanical energy harvesters and touch/acoustic sensors are successfully demonstrated by embedding silver nanowires onto the PPHA-based films. The fabricated devices degrade rapidly under winter sunlight. The degradation rate can be further tuned via changing the ratio of photosensitive agents. This work not only broadens the applicability of TENG as transient power sources and sensors, but also extends the use of transient functional polymers toward advanced energy and sensing applications.

Transient electronics is an emerging class of electronic devices with temporal functional profiles whose degradation can be triggered on demand.[1–4] Such devices can disappear by vaporization, liquefaction, or dissolution in solvents and thus eliminate the need of retrieval after a period of stable operation.[5] They have found potential applications as medical diagnostic and therapeutic devices that can resorb into the body, environmental sensors that do not require recovery after data collection, and consumer devices that can be easily disposed without hazards.[6] The potential feature of disappearance with minimal or non-traceable remains also enables transient electronics to find opportunities in privacy or security applications where stealth is required or reverse engineering needs to be avoided. The transience property is largely attributed to the triggerable degradation of device substrates and encapsulation, which are typically made of a group of materials called transient polymers. Depending on constituting material, the transience can be achieved either through material dissolution or depolymerization. Pioneering efforts on transient electronics focused on solution dissolution of polymer matrix. Bioresorbable polymers such as silk, polycaprolactone, poly(glycolic acid), and poly(L-lactide-*co*-glycolide), were used as substrates,[7–9] and biocompatible, implantable devices such as transistor,[1] ring oscillators,[10] and energy harvesters,[11] have been demonstrated. The lifetime of such devices is controlled by the dissolution rate of the materials in the surrounding aqueous solution, making them unsuitable for non-biological applications.

Dr. C. Wu, Dr. H. Guo, Dr. L. Liu, Dr. W. Ding, Prof. Z. L. Wang
School of Materials Science and Engineering
Georgia Institute of Technology
Atlanta, GA 30332, USA
E-mail: zhong.wang@mse.gatech.edu
Dr. J. Jiang, Prof. P. A. Kohl
School of Chemical and Biomolecular Engineering
Georgia Institute of Technology
Atlanta, GA 30332, USA
The ORCID identification number(s) for the author(s) of this article can be found under https://doi.org/10.1002/aelm.201900725.
X. Pu
Department of Applied Physics
State Key Laboratory of Power Transmission Equipment and System Security and New Technology
Chongqing University
Chongqing 400044, P. R. China
Prof. Z. L. Wang
Beijing Institute of Nanoenergy and Nanosystems
Chinese Academy of Sciences
National Center for Nanoscience and Technology (NCNST)
Beijing 100083, P. R. China

DOI: 10.1002/aelm.201900725

To achieve better control of the device lifetime and expand the utility of transient electronics in non-biological scenarios, the use of metastable polymers whose depolymerization can be triggered rapidly by specific stimuli, has been proposed as an alternative approach for achieving device transience.[5,12] These stimuli can be humidity, heat, light or mechanical stress, and the degradation kinetics can be tuned by material composition. Low-ceiling temperature polymers, which can be kinetically stabilized at room temperature by end-capping or cyclization of polymer chain and depolymerized by backbone bond cleavage under external stimuli, serve as great candidates for transient materials. Among them, cyclic poly(phthalaldehyde) (PPHA) with a low ceiling temperature (T_c = −43 °C) has received broad interest due to its promising mechanical properties, ease of synthesis, and fast depolymerization rates. Diesendruck et al. realized a mechanochemically triggered autonomic remodeling system using high molecular weight PPHA that can go through the depolymerization–repolymerization cycle similar to biological tissues.[13] Tang et al. reported a programmable payload release system from PPHA-based microcapsules, whose release rates could be controlled by the composition and concentration of the salt/acidic methanol solution.[14] When loaded with photosensitive or heat-sensitive agents such as photoacid generator (PAG) or acid-encapsulated wax, PPHA can be depolymerized upon light exposure or thermal treatment. Such PPHA-based substrates have been used for the development of transient resistors, diode/transistor arrays, and organic LEDs.[5,12,15] Transient power sources including both energy storage devices and energy harvesters, however, are indispensable for a fully transient electronic system. To our best knowledge, most of existing reports on transient power sources are about energy storage devices,[16–18] and only transient energy harvesters whose degradation requires aqueous solution have been demonstrated.[4,11,19,20]

Triboelectric nanogenerators (TENGs),[21–23] an emerging mechanical energy harvesting technology with great flexibility in material choices, is promising in offering transient power sources. Here, we reported a TENG whose degradation can be triggered simply and rapidly by sunlight. Its substrate was made of the metastable polymer cyclic PPHA and a photosensitive package (a PAG called Rhodorsil Faba, and a photosensitizer [PS] called anthracene). PS was used to absorb and transfer the energy of ultraviolet light (365–400 nm) to PAG via photo-induced electron transfer, while the latter generated protons to trigger the depolymerization of PPHA. The triboelectric properties of this PPHA-based material were studied and was found to be located between polyurethane and nylon in the triboelectric series. Transient TENG-based mechanical energy harvester and touch/acoustic sensors were successfully demonstrated by coating silver nanowires onto the PPHA-based films. Notably, the fabricated devices can be rapidly degraded in several minutes under winter sunlight, which is much faster than previously reported transient energy harvesters.[4,11,12] The liquid depolymerization byproducts can be quickly absorbed by soil in natural environment and leave minimal traces to avoid detection or reverse engineering. Therefore, this work not only broadens the application of TENG as transient power sources, but also extends the use of transient functional polymers toward advanced energy and sensing applications.

The concept of transient electronics in the field is illustrated in **Figure 1**. The proposed devices can be easily disposed in ambient environment by transforming from solid state into "vanishable" liquid form upon applying an environmental trigger. As a proof of concept, transient TENG-based devices with cyclic PPHA as the substrates were fabricated in this work. As evidenced by the degradation photographs, they could be absorbed by the soil and leave minimal traces within 10 min (actual time taken may vary depending on geographical location, weather conditions, and time of the day) under the sunlight during a typical sunny winter afternoon at Atlanta, USA, whose UV component functioned as the degradation trigger.

Low ceiling temperature, cyclic PPHA was cationically polymerized in dichloromethane (DCM) at −80 °C using boron trifluoride etherate (BF_3OEt_2) as the catalyst. The reaction scheme is shown in **Figure 2**a. The continuous insertion mechanism of monomer, ortho-phthalaldehyde (oPA), into the cyclic structured PPHA, as described in ref. [24], ensured the formation of high molecular PPHA until the reaction equilibrium was achieved. The acetal linkage on the PPHA backbone is highly susceptible to strong acid attack to result in ring-opening of cyclic structure.[25] Upon ring-opening of cyclic PPHA, the end-group unprotected PPHA would rapidly depolymerize back to oPA due to its low ceiling temperature nature. In this study, a superacid (i.e., pK_a less than that of 100% pure sulfuric acid) was in-situ produced upon exposure to UV/visible light using photo-induced electron transfer (PiET) reaction mechanism between anthracene and Rhodorsil FABA.[26] Figure 2b explains the reaction mechanism of PiET reaction. Anthracene acted as a PS to absorb the energy in the ultraviolet spectrum (365–400 nm) while Rhodorsil FABA functioned as a PAG to produce the superacid with proper energy input. The excited PS upon light exposure played the role as an electron donor that can transfer electrons onto a lower energy molecular orbital of PAG due to thermodynamic favorability.[26,27] This redox reaction resulted in the homolytic cleavage of PAG and formation of strong superacid that can rapidly depolymerize the film. All films were casted with addition of an ionic liquid (IL) plasticizer, 1-methylpyrrolidinium bis(trifluoromethylsulfonyl)imide (BMP TFSI). It has been previously reported that pyrrolidinium-based IL can be used to effectively plasticize PPHA film to make it more fracture resistant and flexible.[28–30] Moreover, IL enhances the transient property, due to its good solubility of oPA monomers, resulting in formation of liquid byproducts that can be absorbed into the surrounding environment.

Attenuated total reflectance infrared spectroscopy (ATR-IR) was used to monitor the degradation process of cyclic PPHA film exposed for different length of time, shown in Figure 2c. The neat oPA monomer was investigated as well to find the expected spectrum of depolymerized product. The formation of carbonyl stretching from aromatic aldehyde is expected to be observed around 1670 cm^{-1}. The small peak at around 1720 cm^{-1} corresponded to the carbonyl stretching from carboxylate group from phthalic acid. The formation of phthalic acid was due to the oxidation of oPA after exposing to the humid air. Samples were exposed to an exposure source with an intensity of 4 mW cm^{-2}. At the beginning of exposure, no

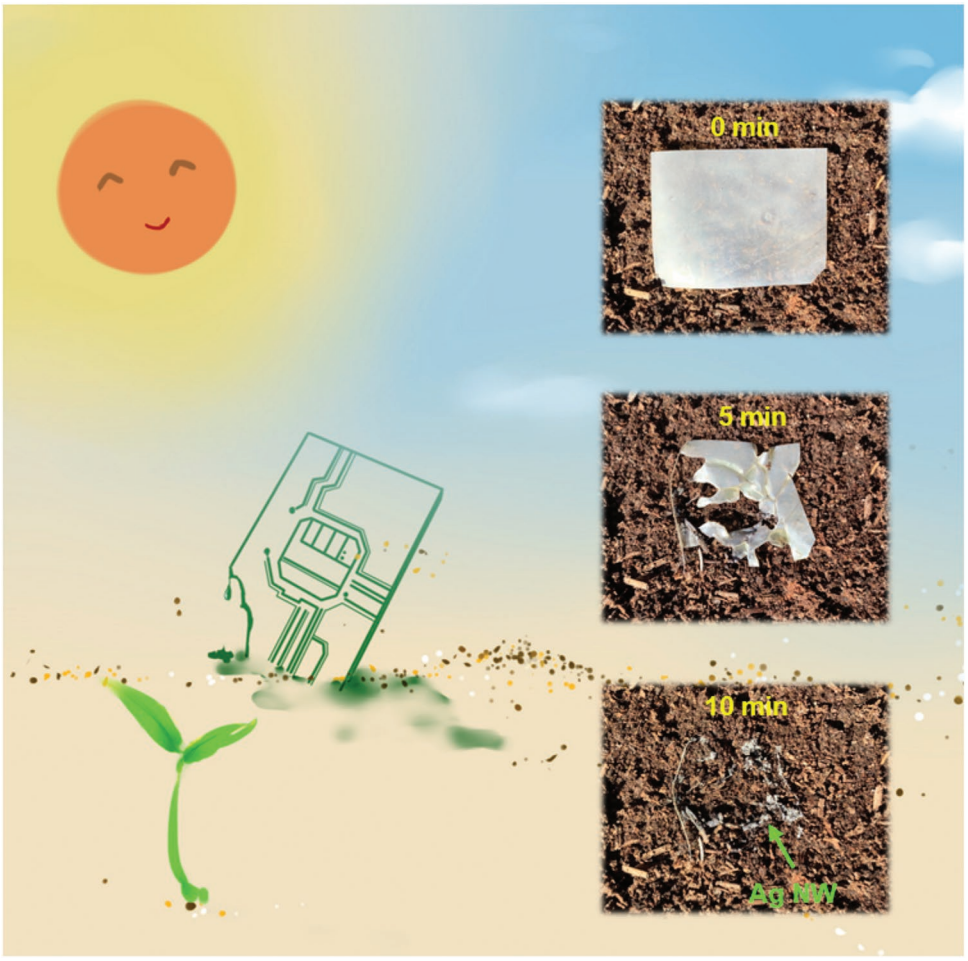

Figure 1. Schematic of transient electronics in the field and photographs of a transient TENG device under sunlight as a proof of concept.

peaks were observed in between 1650 cm^{-1} and 1720 cm^{-1}. With the increase of exposure time, carbonyl stretching from both aromatic aldehyde and carboxylate group became predominant. Exposure for 90 s resulted in complete degradation of cyclic PPHA with a nearly overlapped spectrum with neat oPA monomer. Figure 2d shows the photographs of the degradation process of PPHA. The film started to degrade after 10 s exposure with liquid byproducts started forming on the surface. More liquid appeared on the film surface with the extent of exposure. Upon exposure for 90 s, the surface of the film completely degraded. Further exposure until 300 s resulted in the complete degradation of the film and form liquid byproducts that can be absorbed into the paper background. It is noteworthy that the degradation rate can be further tuned via changing ratio of PAG or by the introduction of weakly basic additive, as elaborated in Supporting Information and another separate report.[30]

TENG has been proven to be an effective tool in characterizing the triboelectric performance, or the ability of capturing surface charges during triboelectrification, of materials.[31] To figure out the position of our PPHA film in the triboelectric series, six contact-separation-mode TENGs[21,23] made of PPHA and different commonly used triboelectric materials, including polyurethane (PU), nylon, polyethylene (PE), polyester (PET), Kapton, and Teflon fluorinated ethylene propylene (FEP), were fabricated (details in Experimental Section) and their electrical outputs are summarized in **Figure 3**. It is noteworthy that the relative position of two materials in the triboelectric series only dictates the direction (signal sign), not the amount, of charge transfer during contact electrification, since the absolute value of TENG output is highly dependent on other factors such as film thickness and material composition as well.[32,33] As in Figure 3a–c, the PU-PPHA TENG generated opposite electrical signals compared to others, which suggests that PU has opposite charge affinity compared to other reference materials when in contact with PPHA. Therefore, a new triboelectric series with PPHA locating between PU and nylon can be obtained, as shown in Figure 3d. The power output of the Kapton-PPHA TENG was measured at various load resistance and it delivered a maximum output power of 28.4 $\mu W\ cm^{-2}$ with a matched resistance of 88 MΩ.

To achieve a fully degradable transient TENG, silver nanowires (Ag NWs), rather than conventional metallic films, were used as the electrode on the PPHA film. The schematic in **Figure 4**a illustrates the fabrication process of the transient TENG, starting with the deposition of Ag NWs on a glass substrate, followed by the deposition of PPHA solution, and ending with the peel-off of the PPHA film coated with Ag

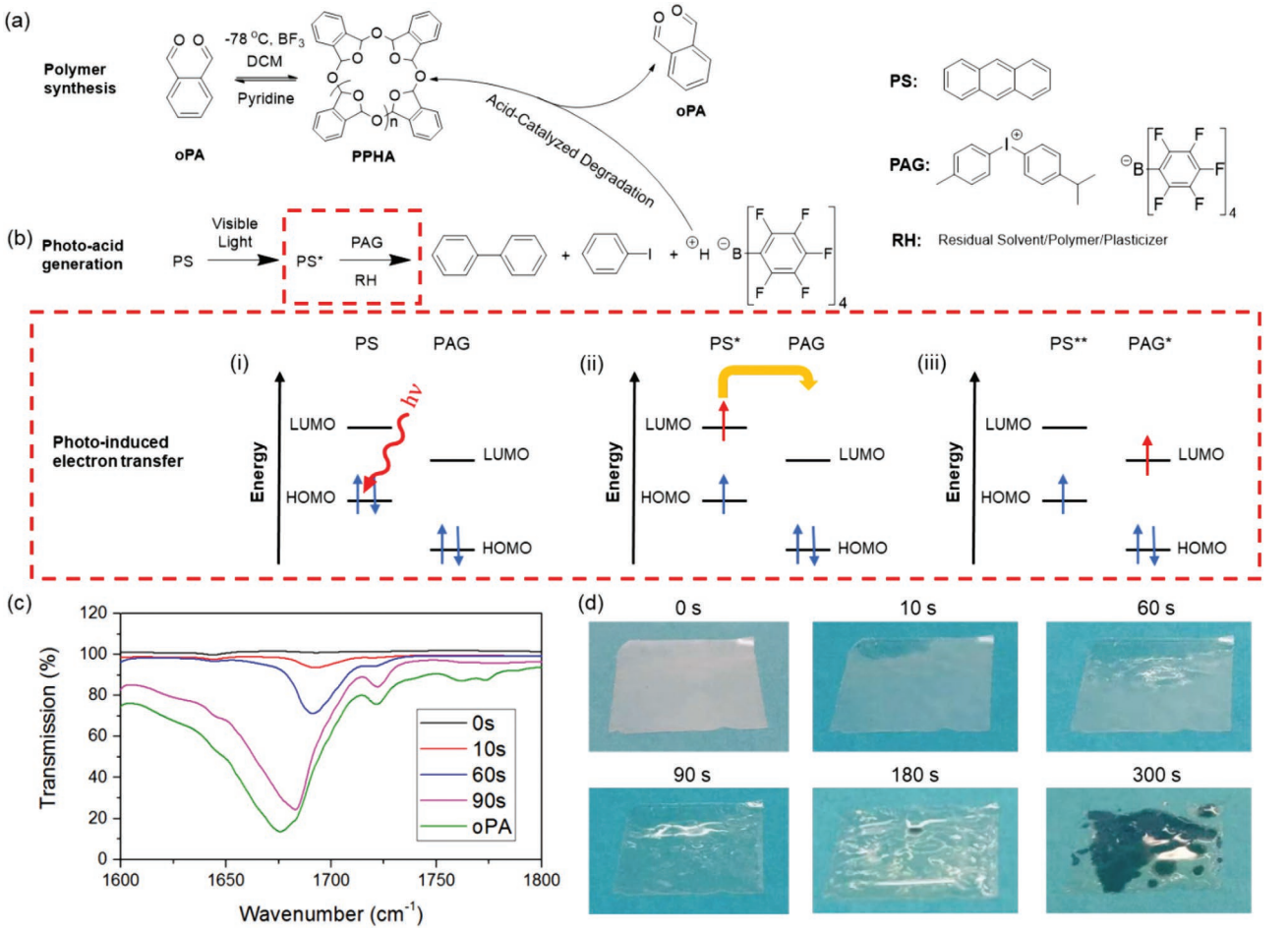

Figure 2. Synthesis and degradation of transient polymer PPHA. a) Cationic polymerization of cyclic PPHA. b) Degradation mechanism of PPHA caused by photo-induced electron transfer reaction. c) In-situ ATR-IR characterization of photo-induced degradation of PPHA. d) Photographs of degradation of PPHA after irradiation under 365 nm UV for various periods of time.

NWs. To characterize its continuous performance under the 365 nm UV irradiation with an intensity of 4 mW cm^{-2}, the temporal profile of V_{OC} of the PPHA-Ag thin film in contact and separation with a copper-coated Kapton film was recorded, with the working mechanism shown in Figure S3a, Supporting Information. The voltage drop from 30 V to 0 V in Figure 4b indicates that its function of electricity generation was attenuated rapidly starting from 30 s UV irradiation and fully disappeared after 90 s. This temporal profile matches well with the observation of the PPHA-Ag film during UV-triggered degradation, as shown in Figure 4c. After 30 s irradiation, the surface of the film started to liquify as evidenced by the change of reflectance when compared to the original film. At 90 s, the whole surface had liquified and the film shape was maintained due to the Ag NWs backbone, which justifies the loss of electrical output as in Figure 4b when solid contact is required for energy conversion. Subsequently, the liquid byproducts were absorbed by the drying agents at the bottom and the solid residue of Ag NWs could be unnoticeable after stirring it with the drying agents. Furthermore, the coating of Ag NWs enhanced the mechanical strength of the PPHA film, with an increase in yield stress from 3.09 to 6.75 MPa and an increase in modulus of resilience from 0.01 J m^{-3} to 0.05 J m^{-3}, while maintaining similar Young's modulus at around 460 MPa, as in Figure S1, Supporting Information. Thermogravimetric analysis (TGA) was also conducted on our PPHA-Ag film to investigate its thermal stability and the result in Figure S2, Supporting Information, shows that the film remained stable up to at 113 °C, well beyond normal ambient temperature.

The as-fabricated PPHA-Ag thin film can work as a single-electrode TENG[34–36] for energy harvesting or sensing upon contact with other materials. The single-electrode mode uses the ground as a reference electrode and can harvest energy from or detect motion of a freely moving object without it being attached to an electrode. This mode greatly reduces the structural complexity of our transient TENG and ensures its full degradability. To demonstrate the electricity generation capability of our transient TENG, it was operated in the single-electrode mode by hand tapping and used to power six light-emitting diodes (LEDs) connected in series. A polytetrafluoroethylene (PTFE) film was attached to the nitrile glove as the other triboelectric material (**Figure 5**a) and the working mechanism is illustrated in Figure S3b, Supporting Information. The LEDs were lit up successfully initially, but after 365 nm UV

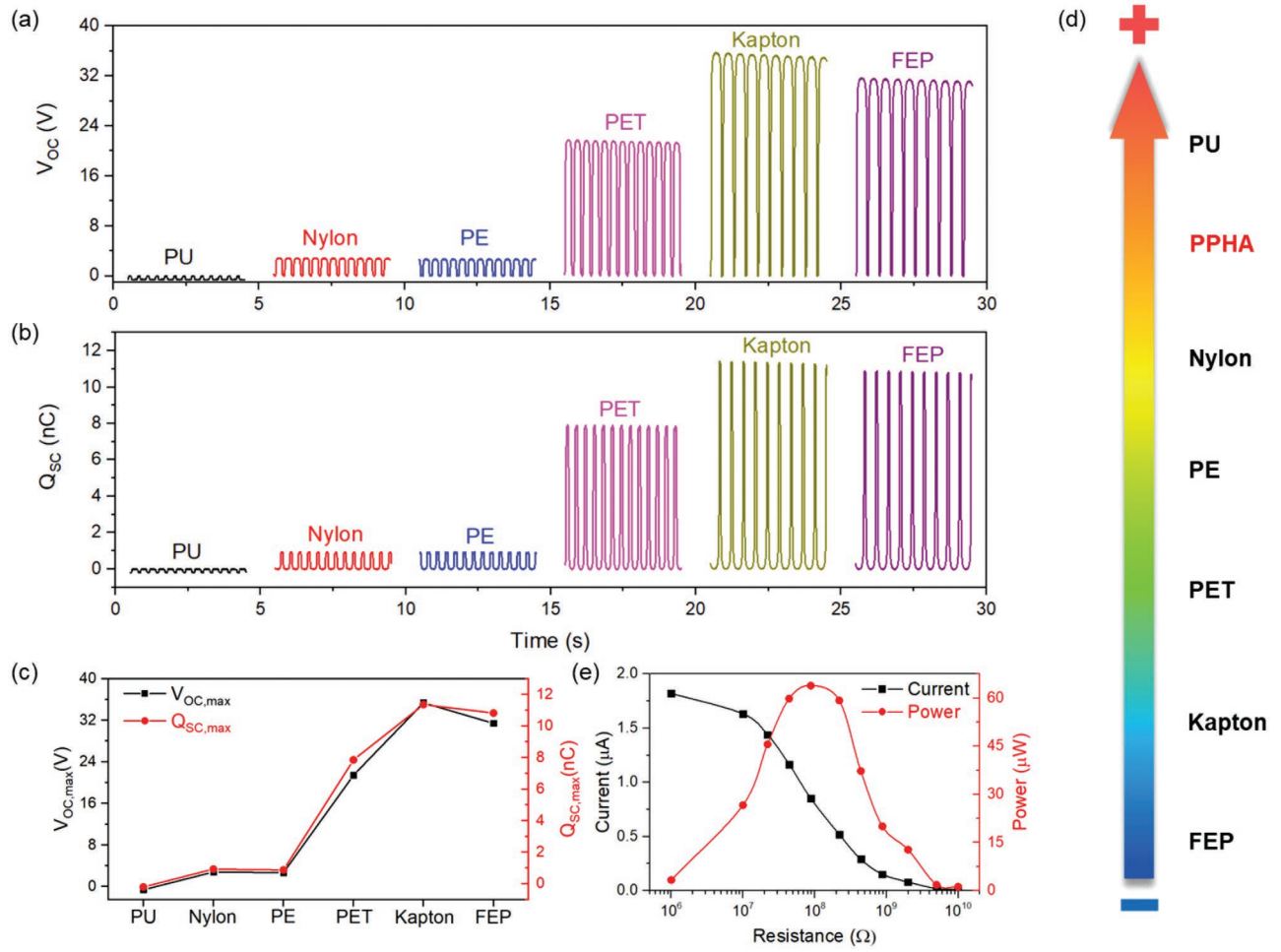

Figure 3. Triboelectric performance of PPHA. a) Open-circuit voltage output V_{OC} and b) short-circuit charge transfer Q_{SC} with respect to different materials. c) Summary of V_{OC} and Q_{SC} data. d) Plot of triboelectric series including PPHA. e) Current and power outputs from a PPHA-Kapton TENG device at various load resistances.

radiation for 2 min, the transient TENG lost the power function due to the liquefaction, as evidenced by the liquid droplets on the PTFE film in Figure 5a. Besides energy harvesting, the transient single-electrode TENG can be used for touch sensing as well. As in Figure 5b and Supporting Information Video, a transient TENG was used as a touch sensor to trigger an alarm bell through a customized control circuit. The bell could be activated by the transient TENG sensor before UV radiation but not after. In Figure 5c, a transient triboelectric acoustic sensor was fabricated by coupling the PPHA-Ag film with a multilayer film consisting of paper, Cu, and Kapton (details can be found in the Experimental Section). The frequency response of the acoustic sensor (100–5000 Hz) is shown in Figure S4, Supporting Information, and it was demonstrated as a microphone to record music played by a speaker, with the output electric signals plotted in Figure 5c. As expected, UV exposure of the device liquified the film and disabled the sound recording function. These demonstrations show that the transient TENG can be "deactivated" via UV/sunlight radiation after their designed use and the resulted liquefaction enables the degradation residue to be easily disposed. Besides, these devices may also be used for secret monitoring in special circumstances.

This work presents a sunlight-triggerable, PPHA-based transient TENG which can be used for both mechanical energy harvesting and active sensing applications. Its degradation is not restricted to aqueous environment and can be achieved with sunlight. The degradation rate can be further tuned via the composition of photosensitive agents. The liquid byproducts after degradation can easily be absorbed by soil or paper with minimal residue remaining, which shows its great potential in field application where disposability or stealth is desired. The adjustment of triboelectric property of PPHA film can be explored in future work by surface modification to achieve higher energy conversion efficiency. This work not only broadens the applicability of TENG as transient power sources and sensors, but also expands the use of transient functional polymers toward advanced energy and sensing applications.

Experimental Section

Materials: Tetrakis(pentafluorophenyl)borate-4-methylphenyl[4-(1-methylethyl)phenyl]iodonium (PAG) were purchased from TCI

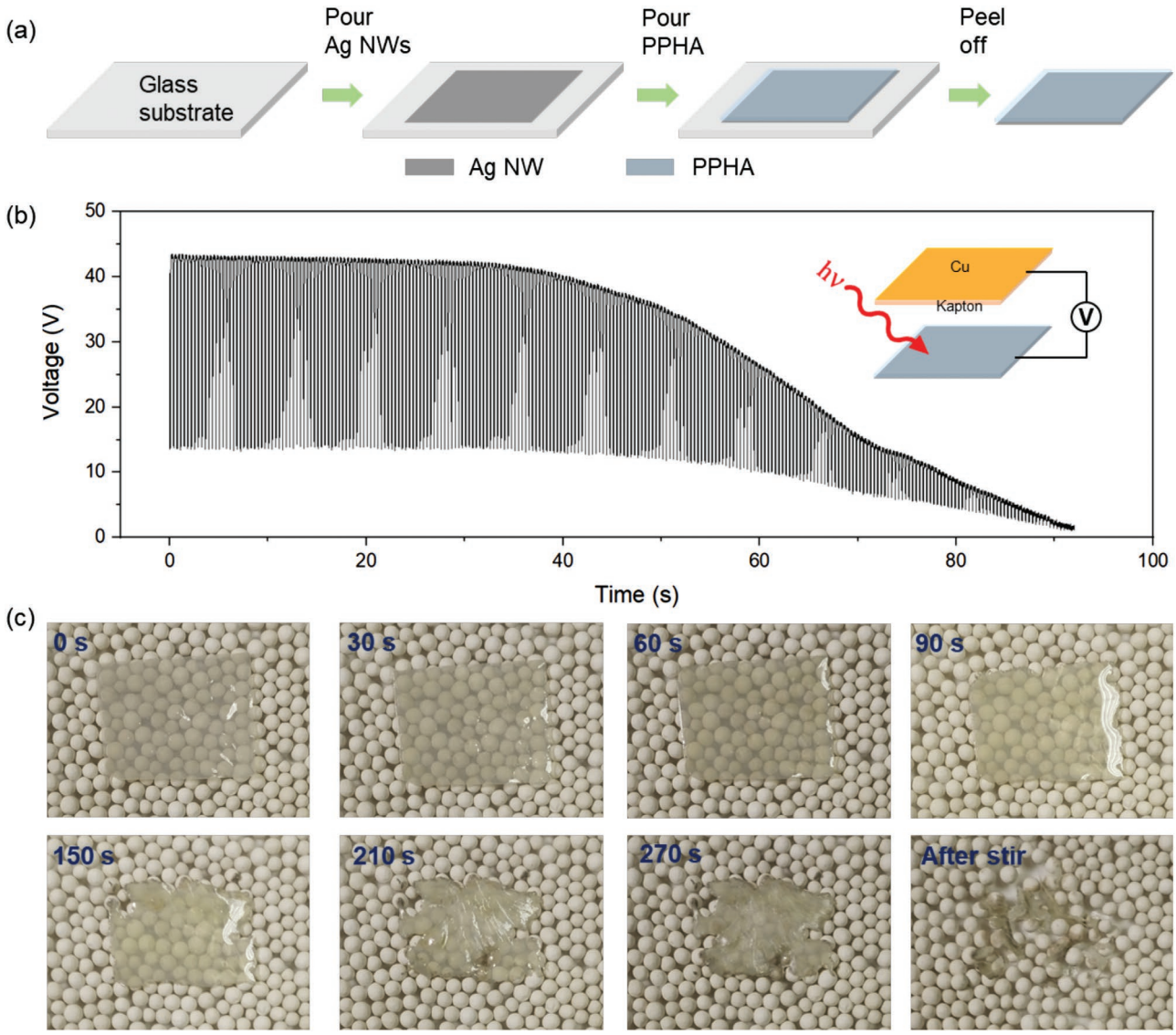

Figure 4. Transient TENG using PPHA and Ag NWs. a) Fabrication process of Ag-NWs coated PPHA thin film. b) Voltage output of the PPHA-Ag thin film in contact and separation with a Cu-coated Kapton film under 365 nm UV irradiation. c) Photographs of degradation of PPHA-Ag thin film after irradiation under 365 nm UV for various periods of time.

Chemicals. Anthracene was purchased from Alfa Aesar. BMP TFSI was purchased from Iolitec. Tetrahydrofuran (THF) was purchased from BDH. All chemicals were used as received. Cyclic PPHA was cationically polymerized using boron trifluoride diethyl etherate (BF_3OEt_2) as the catalyst at −80 °C following the procedure of Schwartz et al.[24] The number-average molecular weight (M_n), weight-average molecular weight (M_w), and polydispersity index ($Đ = M_w/M_n$) of dried cyclic PPHA was determined by gel permeation chromatography (Shimadzu) equipped with an LC-20 CE HPLC pump and a refractive index detector (RID-20 A, 120 V), using THF as the solvent. The measured M_n is 355 kg mol^{-1} and $Đ$ is 1.26. Nylon (50 µm), PE (100 µm), PET (50 µm), and Kapton (25 µm) films were purchased from McMaster-Carr. Teflon FEP film (25 µm) was purchased from American Durafilm. These films were used as received. Waterborne PU dispersion (Bondthane UD-615) was obtained by the courtesy of Bond Polymers International. PU film (50 µm) was made by spin-coating the dispersion onto the substrate. Ag NWs dispersion (Agnw-L70) was purchased from ACS Material. Isopropyl alcohol (IPA) 99% was purchased from VWR.

Fabrication of PPHA Films: PPHA films were formulated in a clean scintillation vial by dissolving all solid contents (i.e., PPHA, PAG, anthracene) and liquid contents (BMP TFSI) in THF. Weight ratio of 12:1 for THF and PPHA were used for all formulations in order to obtain the viscosity to spread and cover the PTFE petri dishes for drying. All polymer formulation was prepared containing 10 part per hundred resin (pphr) PAG, 2.1 pphr anthracene, and 100 pphr BMP TFSI, with all weight fraction referenced to the weight of PPHA added into the formulation. The sample was dried in a nitrogen-rich, pressurized chamber at 15 psig for 18 h, followed by slow bleeding of THF out of chamber to relieve head pressure for 3 h. Samples were then taken out of the pressurized chamber and peeled off the substrate. All samples were then flattened and allowed further drying for 3 days before taken to test. All dried samples have an average thickness of 100 µm.

In-Situ ATR-IR Characterization of PPHA Films: The degradation of 100 µm thick PPHA films was characterized by a Nicolet iS50 FT-IR instrument. ATR mode was used and total scans of 32 were performed for each sample. Samples were exposed using a portable B-100 series

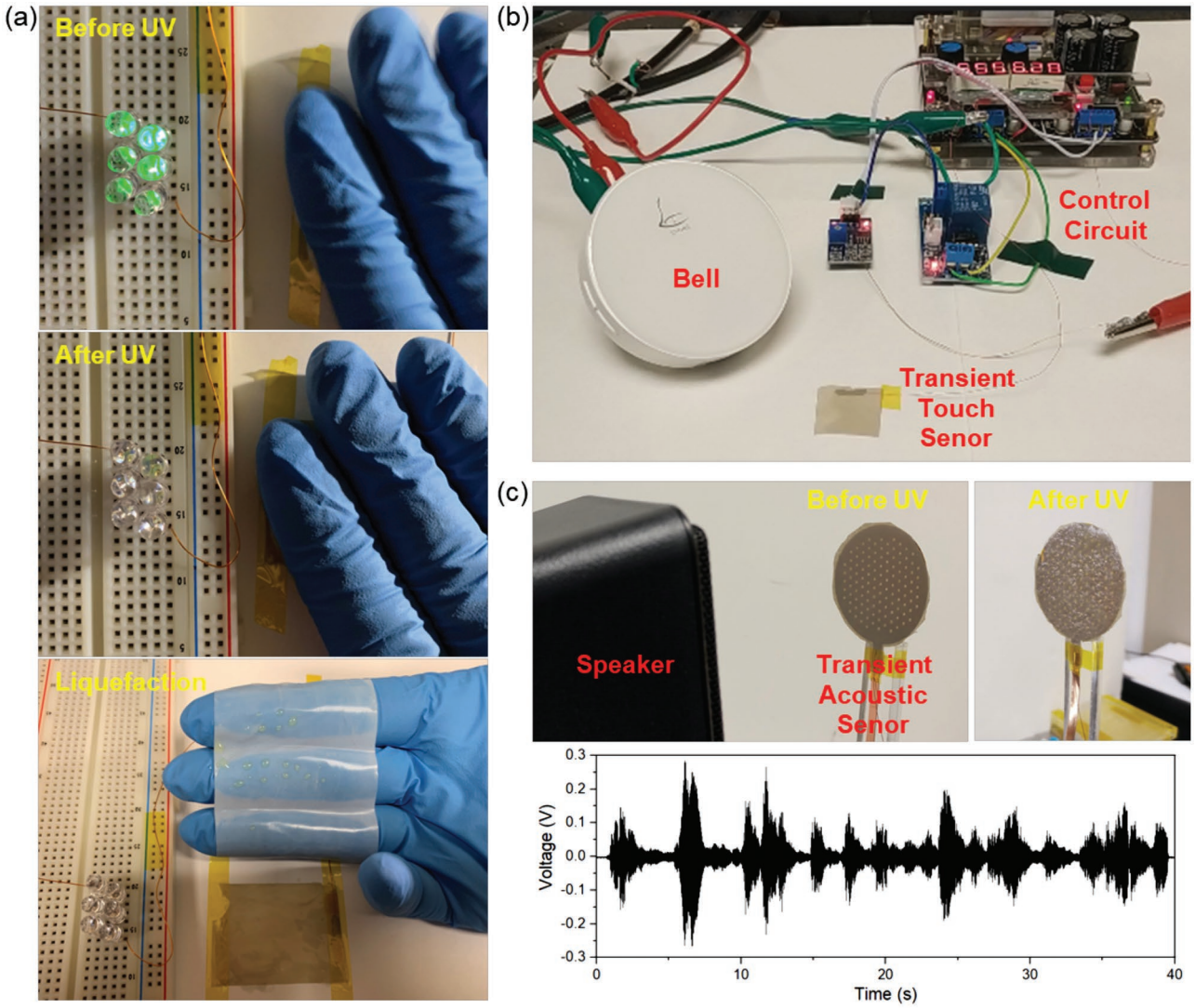

Figure 5. Demonstrations using our transient TENG. a) Electricity generation for lighting up LEDs before UV radiation and the loss of energy harvesting function after UV radiation due to liquefaction. b) Transient touch sensor for alarm triggering. c) A transient triboelectric acoustic sensor and its electrical outputs from music playing.

ultraviolet lamp with an intensity of 4 mW cm^{-2} at 365 nm. Data were collected after samples were exposed for 0, 10, 60, and 90 s. The formation of carbonyl peak at 1680 cm^{-1} were compared to the monomer oPA for indication of the extent of polymer degradation.

Fabrication and Measurement of TENGs for Triboelectric Series: Six TENGs having PPHA and six different reference materials (PU, nylon, PE, PET, Kapton, and FEP) in contact and separation were fabricated to locate the relative position of PPHA in the triboelectric series. Acrylic plates (15 mm wide × 15 mm long × 1/8 inch thick) were used as substrates. For the side with PPHA, the acrylic plates were covered with foam tape, copper tape and PPHA sequentially. For the side with reference materials, the acrylic plates were covered with copper tape and reference materials sequentially. The contact-separation motion between the PPHA and reference materials were driven by a linear motor with a maximum gap distance of 20 mm. The electrical outputs were measured using a Keithley 6514 electrometer.

Fabrication of PPHA-Ag Films: Ag NWs dispersion was first diluted using IPA with a volume ratio of 1:5, and then coated onto clean glass substrates using pipettes. The glass substrates were placed on an optical table overnight to ensure uniform coating of Ag NWs and the complete dry of IPA. Nylon strips were used as fences to create enclosed area on glass substrates to control the surface area and thickness (100 µm) of the casted PPHA layers. PPHA was formulated as described above and uniformly poured into the prepared glass substrates. All films were allowed to dry following the same procedure as described above. The pressure-dried films were allowed for further drying for 24 h in a dark ambient environment. A razor blade was then used to lift off a corner of the PPHA-Ag film from the glass substrate. Films were then submerged into a room-temperature water bath for 15 mins, followed by peeling off the entire film from each glass substrate.

Mechanical Testing of PPHA and PPHA-Ag Films: Mechanical properties of PPHA and PPHA-Ag films were characterized using TA Instrument Q800 Dynamic Mechanical Analyzer. Samples had dimensions of 11 mm × 7 mm × 0.1 mm (length × width × thickness). Stress–strain curves of samples were measured at 23 °C with a preload force of 0.015 N and were elongated with a constant force ramp rate of 1 N min^{-1} until sample-failure occurred, as shown in Figure S1, Supporting Information. Young's modulus [MPa], strain to break value [%], and yield stress [MPa] were obtained from the stress–strain curve. The ability of a material to absorb energy without fracturing is

represented by modulus of resilience [J m−3], which was calculated as $\text{Modulus of resilience} = \frac{\text{Yield stress}^2}{2*(\text{Young's modulus})}$.

Thermal Stability Measurement of PPHA-Ag Film: TGA was performed using a TA Instrument Q50 under inert nitrogen condition with a constant flow rate of 40 mL min^{-1}. Weight of 6.112 mg PPHA-Ag film was loaded into the TGA furnace and investigated for its thermal stability. Furnace temperature was ramped at 5 °C min^{-1} to 250 °C. Figure S2, Supporting Information, shows the weight fraction change of the loaded film with the ramping of temperature. The onset decomposition of the film happened at 113 °C. About 50% residual weight was leftover, due to the residual Ag NWs and non-volatile BMP TFSI.

Measurement of Temporal Voltage Profile of PPHA-Ag Film: A PPHA-Ag film with an area of 15 mm × 15 mm was attached to an acrylic plate with foam cushion and under 365 nm UV irradiation (4 mW cm^{-2}) continuously during the measurement. A Kapton film with copper electrode on an acrylic plate as above was driven by a linear motor to have periodic contact and separation with the PPHA-Ag film, with a maximum gap distance of 20 mm. The V_{OC} was measured using a Keithley 6514 electrometer.

Fabrication of the Transient Acoustic Sensor: A PPHA-Ag film was coupled with a paper sheet covered by Cu and Kapton to form a double-electrode triboelectric acoustic sensor (diameter: 4 cm). Cu was coated onto the paper via evaporation and Kapton film with single-sided adhesive was pasted onto the Cu side of the paper. Uniform holes (diameter: 1 mm; distance: 3 mm) were generated on the paper sheet to reduce air damping during acoustic sensing.[37]

Supporting Information

Supporting Information is available from the Wiley Online Library or from the author.

Acknowledgements

C.W., J.J., and H.G. contributed equally to this work. Research was supported by the Hightower Chair foundation. The authors would like to thank Rieke Metals LLC for scaling cyclic PPHA polymer production and Anthony Engler for GPC characterization for the polymer.

Conflict of Interest

The authors declare no conflict of interest.

Keywords

poly(phthalaldehyde), sensors, transient electronics, triboelectric nanogenerators

Received: July 16, 2019
Revised: September 15, 2019
Published online:

[1] S.-W. Hwang, H. Tao, D.-H. Kim, H. Cheng, J.-K. Song, E. Rill, M. A. Brenckle, B. Panilaitis, S. M. Won, Y.-S. Kim, Y. M. Song, K. J. Yu, A. Ameen, R. Li, Y. Su, M. Yang, D. L. Kaplan, M. R. Zakin, M. J. Slepian, Y. Huang, F. G. Omenetto, J. A. Rogers, *Science* **2012**, *337*, 1640.
[2] S.-W. Hwang, G. Park, H. Cheng, J.-K. Song, S.-K. Kang, L. Yin, J.-H. Kim, F. G. Omenetto, Y. Huang, K.-M. Lee, J. A. Rogers, *Adv. Mater.* **2014**, *26*, 1992.
[3] G. Gourdin, O. Phillips, J. Schwartz, A. Engler, P. Kohl, presented at *IEEE 67th Electronic Components and Technology Conference*, Orlando, FL, May **2017**.
[4] Q. Zheng, Y. Zou, Y. Zhang, Z. Liu, B. Shi, X. Wang, Y. Jin, H. Ouyang, Z. Li, Z. L. Wang, *Sci. Adv.* **2016**, *2*, e1501478.
[5] K. M. Lee, O. Phillips, A. Engler, P. A. Kohl, B. P. Rand, *ACS Appl. Mater. Interfaces* **2018**, *10*, 28062.
[6] S.-W. Hwang, D.-H. Kim, H. Tao, T.-i. Kim, S. Kim, K. J. Yu, B. Panilaitis, J.-W. Jeong, J.-K. Song, F. G. Omenetto, J. A. Rogers, *Adv. Funct. Mater.* **2013**, *23*, 4087.
[7] D.-H. Kim, J. Viventi, J. J. Amsden, J. Xiao, L. Vigeland, Y.-S. Kim, J. A. Blanco, B. Panilaitis, E. S. Frechette, D. Contreras, D. L. Kaplan, F. G. Omenetto, Y. Huang, K.-C. Hwang, M. R. Zakin, B. Litt, J. A. Rogers, *Nat. Mater.* **2010**, *9*, 511.
[8] C. J. Bettinger, Z. Bao, *Adv. Mater.* **2010**, *22*, 651.
[9] H. Acar, S. Çınar, M. Thunga, M. R. Kessler, N. Hashemi, R. Montazami, *Adv. Funct. Mater.* **2014**, *24*, 4135.
[10] S.-W. Hwang, X. Huang, J.-H. Seo, J.-K. Song, S. Kim, S. Hage-Ali, H.-J. Chung, H. Tao, F. G. Omenetto, Z. Ma, J. A. Rogers, *Adv. Mater.* **2013**, *25*, 3526.
[11] C. Dagdeviren, S.-W. Hwang, Y. Su, S. Kim, H. Cheng, O. Gur, R. Haney, F. G. Omenetto, Y. Huang, J. A. Rogers, *Small* **2013**, *9*, 3398.
[12] H. L. Hernandez, S.-K. Kang, O. P. Lee, S.-W. Hwang, J. A. Kaitz, B. Inci, C. W. Park, S. Chung, N. R. Sottos, J. S. Moore, J. A. Rogers, S. R. White, *Adv. Mater.* **2014**, *26*, 7637.
[13] C. E. Diesendruck, G. I. Peterson, H. J. Kulik, J. A. Kaitz, B. D. Mar, P. A. May, S. R. White, T. J. Martínez, A. J. Boydston, J. S. Moore, *Nat. Chem.* **2014**, *6*, 623.
[14] S. Tang, L. Tang, X. Lu, H. Liu, J. S. Moore, *J. Am. Chem. Soc.* **2018**, *140*, 94.
[15] C. W. Park, S.-K. Kang, H. L. Hernandez, J. A. Kaitz, D. S. Wie, J. Shin, O. P. Lee, N. R. Sottos, J. S. Moore, J. A. Rogers, S. R. White, *Adv. Mater.* **2015**, *27*, 3783.
[16] Y. Chen, R. Jamshidi, K. White, S. Çınar, E. Gallegos, N. Hashemi, R. Montazami, *J. Polym. Sci., Part B: Polym. Phys.* **2016**, *54*, 2021.
[17] L. Yin, X. Huang, H. Xu, Y. Zhang, J. Lam, J. Cheng, J. A. Rogers, *Adv. Mater.* **2014**, *26*, 3879.
[18] H. Li, C. Zhao, X. Wang, J. Meng, Y. Zou, S. Noreen, L. Zhao, Z. Liu, H. Ouyang, P. Tan, M. Yu, Y. Fan, Z. L. Wang, Z. Li, *Adv. Sci.* **2019**, *6*, 1801625.
[19] W. Jiang, H. Li, Z. Liu, Z. Li, J. Tian, B. Shi, Y. Zou, H. Ouyang, C. Zhao, L. Zhao, R. Sun, H. Zheng, Y. Fan, Z. L. Wang, Z. Li, *Adv. Mater.* **2018**, *30*, 1801895.
[20] Z. Li, H. Feng, Q. Zheng, H. Li, C. Zhao, H. Ouyang, S. Noreen, M. Yu, F. Su, R. Liu, L. Li, Z. L. Wang, Z. Li, *Nano Energy* **2018**, *54*, 390.
[21] C. Wu, A. C. Wang, W. Ding, H. Guo, Z. L. Wang, *Adv. Energy Mater.* **2019**, *9*, 1802906.
[22] Z. Liu, H. Li, B. Shi, Y. Fan, Z. L. Wang, Z. Li, *Adv. Funct. Mater.* **2019**, *29*, 1808820.
[23] F.-R. Fan, Z.-Q. Tian, Z. L. Wang, *Nano Energy* **2012**, *1*, 328.
[24] J. M. Schwartz, O. Phillips, A. Engler, A. Sutlief, J. Lee, P. A. Kohl, *J. Polym. Sci., Part A: Polym. Chem.* **2017**, *55*, 1166.
[25] M. Tsuda, M. Hata, R. Nishida, S. Oikawa, *J. Polym. Sci., Part A: Polym. Chem.* **1997**, *35*, 77.
[26] O. Phillips, A. Engler, J. M. Schwartz, J. Jiang, C. Tobin, Y. A. Guta, P. A. Kohl, *J. Appl. Polym. Sci.* **2019**, *136*, 47141.
[27] J. V. Crivello, M. Jang, *J. Photochem. Photobiol., A* **2003**, *159*, 173.
[28] J. Jiang, O. Phillips, A. Engler, M. H. Vong, P. A. Kohl, *Polym. Adv. Technol.* **2019**, *30*, 1198.
[29] J. Jiang, M. Warner, O. Phillips, A. Engler, P. A. Kohl, *Polymer* **2019**, *176*, 206.

[30] J. Jiang, O. Phillips, A. Engler, M. H. Vong, P. A. Kohl, *Polym. Adv. Technol.* **2019**, *30*, 1656.
[31] C. Xu, Y. Zi, A. C. Wang, H. Zou, Y. Dai, X. He, P. Wang, Y.-C. Wang, P. Feng, D. Li, Z. L. Wang, *Adv. Mater.* **2018**, *30*, 1706790.
[32] J. Wang, C. Wu, Y. Dai, Z. Zhao, A. Wang, T. Zhang, Z. L. Wang, *Nat. Commun.* **2017**, *8*, 88.
[33] S. Wang, Y. Xie, S. Niu, L. Lin, C. Liu, Y. S. Zhou, Z. L. Wang, *Adv. Mater.* **2014**, *26*, 6720.
[34] C. Wu, X. Wang, L. Lin, H. Guo, Z. L. Wang, *ACS Nano* **2016**, *10*, 4652.
[35] W. Ding, C. Wu, Y. Zi, H. Zou, J. Wang, J. Cheng, A. C. Wang, Z. L. Wang, *Nano Energy* **2018**, *47*, 566.
[36] S. Niu, Y. Liu, S. Wang, L. Lin, Y. S. Zhou, Y. Hu, Z. L. Wang, *Adv. Funct. Mater.* **2014**, *24*, 3332.
[37] H. Guo, X. Pu, J. Chen, Y. Meng, M.-H. Yeh, G. Liu, Q. Tang, B. Chen, D. Liu, S. Qi, C. Wu, C. Hu, J. Wang, Z. L. Wang, *Sci. Rob.* **2018**, *3*, eaat2516.

